Tonic regulation of hippocampal inhibition by endocannabinoids

Ph.D thesis booklet

Benjámin Barti

Semmelweis University
János Szentágothai Doctoral School of Neurosciences

Supervisor:	István Katona, D.Sc
Official Reviewers of the Ph.D. Dissertation:	Katalin Schlett, Ph.D Zoltán Varga, Ph. D
Head of the Final Examination Committee:	Gábor Gerber, D.M.D, Ph.D, C.Sc
Members of the Final Examination Committee:	Márk Kozsurek, M.D, Ph.D Lucia Wittner, D.Sc

Budapest

2024

1. Introduction

Neurotransmission in the brain is achieved through delicate cooperation between distinct molecular machineries, which are segregated into functionally different, spatially aligned nanodomains at both excitatory and inhibitory synapses. Precise and specific arrangement of these molecular complexes allows the fine regulation of the neurotransmitter release probability (Pr), which defines the strength of the synapse. Our quantitative understanding of the molecular architecture that determines anterograde synaptic transmission is rapidly expanding, However, while adjustments of neurotransmitter release also rely on feedback mechanisms from the postsynaptic target cell, the nanoscale functional organization of retrograde synaptic communication remains elusive.

The cannabinoid type-1 receptor (CB_1R) is one of the most abundant G-protein coupled receptors in the brain through which retrograde endocannabinoid (eCB) signaling can alter neurotransmission by both phasic and tonic signaling modalities. Tonic cannabinoid signaling plays considerable role in fine-tuning synaptic strength in cell type-specific and activity-dependent manner. Disruption of tonic cannabinoid signaling is associated with multiple neurological disorders. Despite its physiological and pathological significance, the mechanistic underpinnings and the precise functional organization of the synaptic cannabinoid tone is still enigmatic. While it is known that tonic cannabinoid signaling is cell-type

specific, it is still debated whether 2-arachidonoylglycerol (2-AG) generated by its main synthesizing enzymes diacylglycerol lipase-α (DAGLα), or anandamide (AEA) synthesized by N-acyl phosphatidylethanolamine phospholipase D (NAPE-PLD) is the main ligand of this signaling modality.

Synapses of CB_1R-expressing basket cells (CB_1BCs), which innervate the perisomatic domain of hippocampal CA1 pyramidal cells (PCs) are equipped with molecular cascades which enable both phasic and tonic forms of eCB signaling. As this cell type plays an important role in memory and engram formation, continuous fine adjustment of synaptic Pr between CB_1BCs and PCs via tonic cannabinoid signaling can have profound effects on cell- and network functions. In addition, both short-term and long-term administration of Δ^9-tetrahydrocannabinol (THC) can lead to memory impairment, affecting CB_1R positive inhibitory cells. Therefore, precise understanding of how various forms of endocannabinoid signaling regulates these synapses is essential.

In this regard, our goal was to investigate the role of tonic cannabinoid signaling and define the anatomical and molecular factors and characteristics of CB_1BCs – PC synapses in a cell-compartment- and nanodomain-specific manner. We used patch-clamp electrophysiology in combination with Stochastic Optical Reconstruction Microscopy (STORM), among other techniques, to achieve this.

2. Objectives

Our specific aims are the following:

1) Detailed anatomical and physiological investigation of CB_1BCs and inhibitory synapses specifically present between CB_1BCs and PCs in the hippocampal CA1 region.

- Identification of calcium-binding molecules which can determine unique physiological properties of CB_1BCs.
- Perform electrophysiological and anatomical experiments to study synaptic variability between identified cells.

2) Study the potential role of main molecular components of the endocannabinoid system in tonic cannabinoid signaling at CB_1BC – PC synapses.

- Utilization of multiple transgenic mouse lines in electrophysiological experiments to determine the role of CB_1Rs, together with the major 2-AG and AEA synthetizing enzymes, DAGLα and NAPE-PLD respectively in tonic cannabinoid signaling.

3) Develop a methodological workflow that can address nanoscale molecular principles of tonic cannabinoid signaling in complex brain tissue at CB_1BC – PC synapses.

- Application of *in vitro* paired patch-clamp recordings together with correlated confocal- and super-resolution microscopy to collect electrophysiological, anatomical and nanoscale molecular data from the very same synapse in acute brain slice preparations.
- Test the hypothesis with multiple *in vivo* perturbation models including modest genetic ablation of CB_1Rs and chronic administration of THC.

3. Methods

3.1. Animals

In electrophysiological, anatomical, and analytical experiments C57Bl/6J male mice (postnatal day 27 - 45) were used, together with strains containing genetic deletion of specific protein coding genes: CB_1R knockout (KO) (provided by A. Zimmer), DAGLα KO (provided by K. Sakimura), NAPE-PLD KO (provided by B. Cravatt). In cases where genetically modified mice were used, their wild-type littermates were utilized for control measurements. For chronic drug treatment, male C57BL/6J mice (postnatal day 22–31) were injected twice daily intraperitoneally with vehicle (1% ethanol, 2% Tween 80 and saline) or THC for 6.5 days.

3.2. Electrophysiological experiments

All electrophysiological recordings from interneuron and pyramidal cell pairs were made in a submerged recording chamber at 33°C constantly perfused with oxygenated artificial cerebrospinal fluid (ACSF) solution, using micropipettes (3–4 MΩ resistance). Electrophysiological properties of CB_1BCs and postsynaptic inhibitory currents on PCs were recorded in whole-cell patch-clamp configuration. During each experiment interneurons were labeled via 0.2% biocytin to allow *post-hoc* morphological analysis, while in certain experiments PCs were also labeled with Cascade Blue hydrazide, trisodium salt included in the intracellular solution. In pharmacological experiments, AM251

was used as a CB_1R antagonist/inverse-agonist, to block CB_1R activity. To examine acute drug effects bath ACSF was changed to drug-ACSF solution (containing 10 μM AM251) after the baseline was recorded for at least 5-10 minutes.

3.3. Immunostaining

Fluorescent immunolabeling was used throughout the study to visualize single- or multiple labeled individual cells and protein distributions in brain slices. All tissue samples were stained free-floating, in 24-well tissue culture dishes. The following primary antibodies were used: Bassoon (mouse, 1:2000, Abcam), AF-405/Cascade Blue (rabbit, 1:1000, Thermo Fisher Scientific), CB_1 (guinnea pig, 1:2000, Gift of M. Watanabe), CB_1 (rabbit, 1:2000, ImmunoGenes), NECAB1 (rabbit, 1:300, Atlas Antibodies), NECAB2 (rabbit, 1:500, Atlas Antibodies), Parvalbumin (goat, 1:4000, Swant). Labeled fluorescent secondary antibodies were purchased from Jackson ImmunoResearch. After electrophysiological recordings, single-labeled interneuron-containing 300 μm-thick slices were washed three times in 0.1 M Phosphate-buffer (PB) for 10 minutes and treated with 0.5% Triton-X100 in 0.1 M PB together with 10% normal donkey serum (NDS) in 0.1 M PB for 30 minutes. Slices were incubated with streptavidin conjugated to DyLight-488 for 2 hours to visualize biocytin. After washing the slices three times with 0.1 M PB for 10 minutes, samples were mounted on glass slides in Vectashield coverslipped, and sealed with nail polish. After confocal

imaging of cellular morphology, 300 μm-thick sections were first returned to PB and then embedded in 2% agarose in distilled water for resectioning. 10 - 20 μm-thick sections were cut with a Leica VT-1000S Vibratome, then after extensive slices were treated with a solution containing 5% NDS and 0.1% Triton X-100 in Tris-buffered saline (TBS) for 45 minutes, followed by incubation in the TBS-solution of the primary antibodies overnight at room temperature. On the following day samples were thoroughly washed and incubated in the TBS-solution of the fluorescently-labeled secondary antibodies for 4 hours. Finally, samples were washed in TBS and PB, then mounted either in Vectashield for confocal imaging or in imaging medium containing 5% glucose, 0.1 M 2-Mercaptoethylamine, 1 mg/ml glucose oxidase (Sigma) and 1500 U/ml catalase (Sigma) in Dulbecco's phosphate buffered saline for super-resolution imaging.

3.4. Microscopy

To assess interneuron morphology, 20x-magnification z-stacks (with 1 μm step size in z direction) and maximal intensity z-projections of recorded cells were collected from 300 μm-thick sections on a Nikon A1R confocal scan head coupled to a Nikon Ti-E inverted microscope (Nikon Instruments, Japan) using a CFI Plan Apo VC 20x objective (NA: 0.75 NA). In order to visually identify close anatomical appositions of those paired recordings in which the pyramidal cells were also labeled, 60x-magnification objectives were used (CFI Plan Apo VC 60X Oil; NA:

1.4) together with appropriate Nyquist-sampling (pixel size = 0.14 μm/px, z-step = 0.125 μm) to capture high-resolution z-stacks. The same microscope and objectives were used to obtain high-resolution z-stacks of fluorescent immunostainings in hippocampus. Confocal images of Cascade Blue, biocytin, bassoon and CB_1R, and Stochastic Optical Reconstruction Microscopy (STORM) images of CB_1R, were captured on a Nikon N-STORM system with a 100x TIRF objective (1.49 NA). In STORM mode, z-stacks of 7 3D-STORM movies allowed highly homogenous sampling of the volume over 1000 nm slice thickness. For each imaged bouton, the confocal and STORM images of CB_1R were first aligned manually, and CB_1R LPs belonging to the bouton were selected in 2D using VividSTORM.

3.5. Quantification, statistical analysis and figure preparation

The obtained data from the different experiments were statistically analyzed and graphs were generated using GraphPad Prism 10 (GraphPad Software, San Diego, CA, USA). Sample sizes were estimated based on previous experience and were similar to those generally applied in the field. For figure preparation Adobe Photoshop and Illustrator (Adobe Inc., San Jose, CA, USA) were used.

4. Results

4.1 Target cell-dependent variability of CB_1BC – PC synapses.

CB_1BC – PC connections exhibit large variability in terms of the number of putative anatomical connections, the amplitude and the number of successful inhibitory postsynaptic currents (IPSCs). The average connection number between pairs was 2.7 ± 1.5, although, there were pairs that contained only 1 or 9 close anatomical appositions as well. Surprisingly, the number of anatomical connections only showed weak correlation with the IPSC amplitudes and successes (n = 55 pairs, IPSC: r = 0.25, p_{ns} = 0.06, successes: r = 0.33, *p = 0.01, Spearman's rank-order correlation). These results arise from the variations of these properties which are profound even when there are similar numbers of connections between cells. To determine whether the synapse-specific fine-tuning of the synaptic weights of CB_1BC synapses is primarily driven by the pre- or the postsynaptic neuron, we performed sequential paired whole-cell patch-clamp recordings where multiple postsynaptic PC pairs were investigated for a single presynaptic interneuron. These experiments showed similar results (n = 22 pairs, IPSC amplitude: r = 0.002, p_{ns} = 0.99, successes: r = 0.02, p_{ns} = 0.91, Spearman's rank-order correlation). These observations suggest that the efferent synapses of a single CB_1BC exhibit large differences in their synaptic weights in a postsynaptic target cell-dependent manner.

Intracellular Ca^{2+}-buffering proteins can also have a major effect on the electrophysiological properties of the neurons. *In silico* data analysis revealed that CB_1BCs express two major understudied Ca^{2+}-buffer proteins: N-terminal EF-hand Calcium Binding Protein 1 and 2 (NECAB1/2). Therefore, we studied the anatomical localization of these proteins in individual filled CB_1BCs to see whether they can differentially regulate release properties. We found that these proteins are localized in distinct cellular domains: NECAB1 expression was prominent in the somatodendritic domain of the interneurons, while NECAB2 was also present at the axon terminals. Taken together, the subcellular compartment-specific differences between NECAB1 and NECAB2 proteins indicate that these calcium-binding proteins could fulfill multiple functionally different roles in the regulation of Ca^{2+}-signaling dynamics.

4.2. Tonic endocannabinoid signaling fine-tunes synaptic transmission.

In basal conditions tonic cannabinoid signaling consistently fine-tunes CB_1BC – PC synapses which can influence Pr and affect synaptic strength. We conducted paired recordings on CB_1R WT and KO mice samples, where AM251 (a CB_1R antagonist/inverse agonis) was applied to block CB_1R activity and reveal the magnitude of tonic cannabinoid signaling. Indeed, while on CB_1R WT samples the IPSC amplitudes and successes were increased after AM251 application, in KO samples there

were no significant change in these parameters (CB_1R WT: n = 11 pairs, amplitudes: **p = 0.006, successes: ***p=0.0003, CB_1R KO: n = 12 pairs, amplitudes: p_{ns} = 0.86; successes: p_{ns} = 0.25, Two-way ANOVA with repeated measures). In KO samples the coefficient of variation (CV) of baseline IPSC peaks were decreased compared to WT values (*p = 0.03), which indicate that tonic cannabinoid signaling affects synaptic variability by 33.6 ± 10.7% thus, substantially influencing target cell-dependent synaptic variability.

4.3. DAGLα-, NAPE-PLD-independent tonic cannabinoid signaling fine-tunes synaptic transmission at CB_1BC – PC synapses.

Next, we aimed to investigate which of the two main endocannabinoid lipids regulate tonic cannabinoid signaling at these synapses. We utilized genetically modified mice strains where either DAGLα or NAPE-PLD, the main synthesizing enzymes of 2-AG and AEA, respectively, were absent. Interestingly, paired recordings showed intact tonic cannabinoid signaling in both experiments: AM251 increased the IPSC amplitudes and successes in both KOs, similar to WT littermates (DAGLα KO: n = 12 pairs, amplitudes: *p = 0.03, successes: *p = 0.004; NAPE-PLD KO: n = 7 pairs, amplitudes: *p = 0.04, successes: **p = 0.003, Two-way ANOVA with repeated measures). These findings demonstrate that there is a DAGLα-, NAPE-PLD-independent form of tonic cannabinoid signaling at this synapse type.

4.4. Nanoscale CB_1R/effector stoichiometry determines tonic cannabinoid signaling.

As depletion of either 2-AG or AEA endocannabinoid lipids does not influence tonic cannabinoid signaling, we investigated CB_1R distributions. CB_1Rs also have constitutive activity at these synapses therefore, we reasoned that if constitutive CB_1R activity contributes to the synaptic cannabinoid tone, then the molecular abundance of CB_1Rs within the close proximity of the synaptic area should predict the magnitude of the cannabinoid tone. To test this hypothesis directly, we developed a workflow in which beside the measurement of physiological parameters from unitary synaptic connections, correlative morphological data, and nanoscale-level molecular distribution of receptors were also available within complex brain tissue (Figure 1).

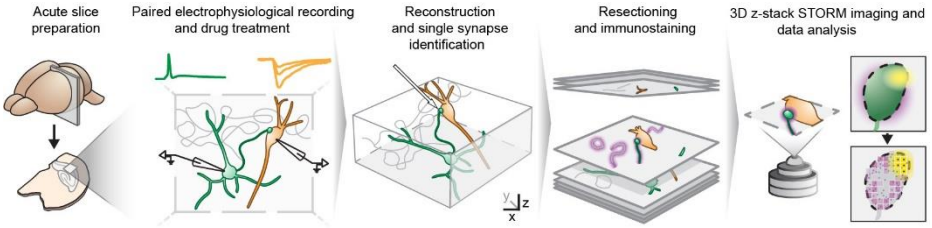

Figure 1. Correlated electrophysiological, anatomical and nanoscale molecular analysis of unitary CB_1BC - PC synapses.

We carried out paired recordings from CB_1BCs and CA1 PCs, and recorded IPSCs before and after AM251 application to measure the magnitude of the synaptic cannabinoid tone. The presynaptic basket cell and the postsynaptic PC were filled with biocytin and Cascade Blue, respectively. The neuronal processes were anatomically reconstructed at high magnification to determine all synaptic connections. Since variance-mean experiments by us and others revealed that even in a single bouton with a single active zone there might be multiple release sites we focused on pairs that were connected with a single synapse and contained one confocal bassoon cluster (identified via neighboring bassoon positive voxels on the confocal image) located opposite to the postsynaptic neuron. These connections were selected for STORM imaging. The z-stack image of the synaptic connection was acquired by volumetric 3D-STORM super-resolution imaging to visualize the synapse regardless of bouton orientation. CB_1R nanoscale density was calculated in relation to the active zone visualized by bassoon-immunolabeling and Pr was estimated from recorded successes. Correlated measurements of the estimated Pr, the active zone size, and the number of CB_1Rs along the entire bouton surface revealed that the total CB_1R number on the axon terminal or bassoon voxel numbers does not predict Pr (n = 9 pairs, total CB_1R number: r = 0.05, p_{ns} = 0.90, bassoon: r = 0.05, p_{ns} = 0.90). When the nanoscale stoichiometry parameter was calculated by measuring the ratio of intra/perisynaptic CB_1Rs and bassoon-positive voxels, we found a strong inverse correlation with the estimated release probability (r = -

0.74, *p = 0.03). The correlative relationship depends on the persistent activity of intra/perisynaptic CB_1Rs, because AM251 administration on the same pairs eliminated the correlation between the receptor/effector ratio and the Pr ($r = -0.05$ $p_{ns} = 0.90$). In addition, Pr also scales with the effect of AM251 ($r = -0.8$, *p = 0.01, Spearman rank-order correlation). In other words, the more intra/perisynaptic CB_1Rs control the release machinery, the larger the impact of synaptic cannabinoid tone on Pr.

4.5. Selective reduction of extrasynaptic CB_1R abundance does not affect the cannabinoid tone.

If nanodomain-specific CB_1R activity is indeed responsible for the synaptic cannabinoid tone, then selective perturbation of intra- versus extrasynaptic CB_1R abundance would differentially affect this synaptic phenomenon. Therefore, next, we investigated whether perturbations that change CB_1R density can affect tonic cannabinoid signaling. In CB_1R heterozygous mice (HET), CB_1R protein levels were reduced by half in cortical areas including the hippocampus compared to WT littermates (n = 3 animals/genotype, *p = 0.04 one-way ANOVA with Dunnett`s multiple comparisons test). Moreover, CB_1R STORM imaging also showed a strong reduction in the number of localization points representing CB_1Rs along the entire bouton surface in HET mice (***p < 0.0001, Mann-Whitney U test). In contrast, CB_1R numbers in the nanoscale vicinity of bassoon clusters were similar in both genotypes,

suggesting that axon terminals first fill up the intra/perisynaptic CB_1R population (0-200 nm: p_{ns} = 0.08, Mann-Whitney U test). Notably, despite the marked reduction in CB_1R levels in HET samples, paired recordings showed no difference in terms of tonic cannabinoid signaling compared to WT (HET: n = 9 pairs, amplitudes: **p = 0.003, successes: *** p < 0.0001, Two-way ANOVA with repeated measures).

4.6. *In vivo* THC administration disrupts presynaptic nanoscale stoichiometry and the synaptic cannabinoid tone.

Previously, it was shown that Δ^9-tetrahydrocannabinol (THC), a psychoactive compound in marijuana reduces the CB_1R numbers on perisomatic bouton surface. However, our findings in HET mice revealed that a robust reduction of CB_1Rs in axon terminals measured at the microdomain level may not necessarily have functional consequences on synaptic transmission. Conversely, if THC exposure compromises the intrasynaptic nanoscale stoichiometry, it would also alter the cannabinoid tone. To address this question, we applied *in vivo* THC treatment in mice which was followed by *ex vivo* electrophysiological and anatomical investigation of CB_1BC boutons with correlated confocal and STORM imaging. These experiments showed unaltered boutonal morphology and active zone size, but the reduction of CB_1Rs on the bouton surface followed by THC administration also affected the intra/perisynaptic nanodomain besides extrasynaptic CB_1Rs (0-200 nm: **p = 0.002,

Mann-Whitney U test). In line with our hypothesis, paired patch-clamp recordings revealed an impaired tonic cannabinoid signaling compared to vehicle treated group (vehicle: n = 11 pairs, amplitudes: ***p = 0.0004, successes: ***p < 0.0001; THC: n = 11 pairs, amplitudes: p_{ns} = 0.18, successes: p_{ns} = 0.74, Two-way ANOVA with repeated measures). Moreover, THC treatment also reduced the CV of IPSC peak amplitudes recorded during baseline between groups (**p = 0.004). These findings demonstrate that THC exposure impairs the precise nanoscale functional organization that underlies the synaptic cannabinoid tone and reduces the synapse-specific variability of CB_1BC output synapses. Our results also highlight the importance of nanodomain-specific measurements for providing physiologically and pathologically relevant insights into drug-induced molecular changes.

5. Conclusions

In this study, we show that a specific form of retrograde cannabinoid signaling is essential for setting target cell-dependent synaptic variability at hippocampal inhibitory synapses. Importantly, it does not require the activity of the two major endocannabinoid-producing enzymes diacylglycerol lipase-α (DAGLα) and N-acyl phosphatidylethanolamine phospholipase D (NAPE-PLD). By developing a workflow for the measurement of physiological, anatomical, and molecular parameters at the same unitary synapse, we demonstrate that the nanoscale stoichiometric ratio of CB_1 receptors (CB_1R) to the release machinery is sufficient to predict synapse-specific release probability. Accordingly, selective extrasynaptic CB_1R reduction does not affect synaptic transmission, whereas *in vivo* treatment by Δ^9-tetrahydrocannabinol (THC) disrupts the intrasynaptic nanoscale stoichiometry and reduces synaptic variability. Our results imply that synapses leverage the nanoscale stoichiometry of presynaptic receptor coupling to the release machinery to establish synaptic strength in a target cell-dependent manner. These findings provide insights into the molecular tolerance mechanisms underlying cannabis use disorder and highlight that nanodomain-specific molecular imaging is essential to understand the physiological consequences of drug effects.

6. List of publications

Publications related to this thesis

Barti, B., Dudok, B., Kenesei, K., Zöldi, M., Miczán, V., Balla, G. Y., Zala, D., Tasso, M., Sagheddu, C., Kisfali, M., Tóth, B., Ledri, M., Vizi, E. S., Melis, M., Barna, L., Lenkei, Z., Soltész, I., and Katona, I. (2024). Presynaptic nanoscale components of retrograde synaptic signaling. Sci. Adv., 10(22). https://doi.org/10.1126/sciadv.ado0077

Miczán, V., Kelemen, K., Glavinics, J. R., László, Z. I., **Barti, B.**, Kenesei, K., Kisfali, M., and Katona, I. (2021). Necab1 and necab2 are prevalent calcium-binding proteins of cb1/cck-positive gabaergic interneurons. *Cereb. Cortex*, *31*(3), 1786–1806. https://doi.org/10.1093/cercor/bhaa326

Other publications

Kis, V., **Barti, B.**, Lippai, M., & Sass, M. (2015). Specialized cortex glial cells accumulate lipid droplets in Drosophila melanogaster. *PloS one*, *10*(7). https://doi.org/10.1371/journal.pone.0131250

Prokop, S., Ábrányi-Balogh, P., **Barti, B.**, Vámosi, M., Zöldi, M., Barna, L., Urbán, G. M., Tóth, A. D., Dudok, B., Egyed, A., Deng, H., Leggio, G. M., Hunyady, L., van der Stelt, M., Keserű, G. M., and Katona, I. (2021). PharmacoSTORM nanoscale pharmacology reveals cariprazine binding on Islands of Calleja granule cells. *Nat. Commun.*, *12*(1), 1–19. https://doi.org/10.1038/s41467-021-26757-z